Accepted Article

Redox proteomic analysis reveals oxidative modifications of proteins by increased levels of intracellular reactive oxygen species during hypoxia adaptation of *Aspergillus fumigatus*

Elena Shekhova*, Lia Ivanova, Thomas Krüger, Maria C. Stroe, Juliane Macheleidt, Olaf Kniemeyer#, Axel A. Brakhage

Department of Molecular and Applied Microbiology, Leibniz Institute for Natural Product Research and Infection Biology – Hans Knöll Institute (HKI), and

Department of Microbiology and Molecular Biology, Institute of Microbiology, Friedrich Schiller University, Jena, Germany

*Current address: Medical Research Council Centre for Medical Mycology at the University of Aberdeen, Institute of Medical Sciences, Foresterhill, Aberdeen, UK

Running title: Hypoxia adaptation of *Aspergillus fumigatus*

Received: 09 11, 2018; Revised: 12 20, 2018; Accepted: 01 09, 2018

This article has been accepted for publication and undergone full peer review but has not been through the copyediting, typesetting, pagination and proofreading process, which may lead to differences between this version and the Version of Record. Please cite this article as doi: 10.1002/pmic.201800339.

This article is protected by copyright. All rights reserved.

#Address correspondence to Olaf Kniemeyer, Leibniz Institute for Natural Product Research and Infection Biology – Hans Knöll Institute, Adolf-Reichwein-Str. 23. 07745 Jena, Germany; Fax: +49 3641 532 2071, E-mail: olaf.kniemeyer@leibniz-hki.de

Accepted Article

This article is protected by copyright. All rights reserved.

Accepted Article

List of abbreviations:

Af, *Aspergillus fumigatus*; AGC, automatic gain control; AMM, Aspergillus minimal medium; AspGD, Aspergillus genome database; FunCat, functional catalogue; FWHM, full width at half maximum; GFP, green fluorescent protein; HCD, higher-energy collisional dissociation; HIF-1, Hypoxia-inducible factor; IAM, iodoacetamide; NCE, normalised collision energy; NO, Nitric oxide; PRIDE, proteomics identification; PSMs, Peptide spectral matches; tBOOH, tert-butylhydroperoxide; TCEP, tris(2-carboxyethyl)phosphine; TEAB, triethylammonium bicarbonate; TMT, tandem mass tag

Keywords: iodoTMT, Coa6, hypoxia, ROS, Yap1, redox homeostasis

Total number of words: 7377

This article is protected by copyright. All rights reserved.

Accepted Article

Abstract

At the site of infection, the human fungal pathogen *Aspergillus fumigatus* faces abrupt changes in oxygen concentrations. An increasing number of studies have demonstrated that elevated production of intracellular reactive oxygen species (ROS) under low oxygen conditions plays a regulatory role in modulating cellular responses for adaptation to hypoxia. To learn more about this process in *A. fumigatus*, we determined intracellular ROS production during hypoxia. Our results confirmed increased amounts of intracellular ROS in *A. fumigatus* exposed to decreased oxygen levels. Moreover, nuclear accumulation of the major oxidative stress regulator AfYap1 was observed after low oxygen cultivation. For further analysis, we applied iodoTMT labelling of redox-sensitive cysteine residues to identify proteins that are reversibly oxidised. This analysis revealed that proteins with important roles in maintaining redox balance and protein folding, such as the thioredoxin Asp f 29 and the protein disulphide PdiA, underwent substantial thiol modification under hypoxia. Our data also showed that the mitochondrial respiratory complex IV assembly protein Coa6 was significantly oxidised by hypoxic ROS. Deletion of the corresponding gene resulted in a complete absence of hypoxic growth, indicating the importance of complex IV during adaptation of *A. fumigatus* to oxygen-limiting conditions.

This article is protected by copyright. All rights reserved.

Accepted Article

Statement of Significance

The ubiquitous filamentous fungus *Aspergillus fumigatus* causes a wide spectrum of diseases in humans. In dependence on the immune status of the host, these diseases range from allergic asthma, to chronic lung colonisation and life-threatening, invasive infections, which all predominantly occur in the lungs. Interestingly, previous studies have shown that *A. fumigatus* is exposed to low oxygen levels during pulmonary infection. Here, we characterized the proteomic response of *A. fumigatus* to a short period of hypoxia by LC-MS/MS-based detection of relative changes in protein abundances and redox-dependent cysteine modifications. Our study revealed several important findings. The intracellular production of ROS increases in response to oxygen depletion. These hypoxia-induced ROS activate the oxidative stress response via the global transcriptional regulator AfYap1, and moreover, trigger the oxidation of cysteine thiols in a subset of proteins. This includes, among others, the cytochrome c oxidase assembly factor 6 that is required for the biogenesis of the copper redox centre in the mitochondrial respiratory complex IV. We show that its absence impedes hypoxic growth. Thus, maintenance of the operability of complex IV is essential for hypoxic survival.

This article is protected by copyright. All rights reserved.

Accepted Article

1. Introduction

Infections caused by the fungal pathogen *Aspergillus fumigatus* represent a growing problem in immunocompromised and critically ill patients. The inhaled *A. fumigatus* spores are able to cause a life-threatening mycosis, referred to as invasive pulmonary aspergillosis [1]. *A. fumigatus* also contributes to chronic lung infections in patients with pulmonary pathologies such as cystic fibrosis [2]. The threat of *A. fumigatus* infections is aggravated by difficult diagnosis and the limited number of available therapeutic antifungal strategies. Therefore, a better understanding of the infection process including novel fungal-specific molecular targets, which can be inhibited to prevent a fungal infection, is urgently needed.

A. fumigatus lung infections are characterised by several stages, including spore transmission into the airways by inhalation, germination, and hyphal growth into the lung tissue. Patients are typically diagnosed and treated with antifungals only at the later stages of a fungal infection, when *A. fumigatus* hyphae have already invaded the lung. Thus, the investigation of cellular pathways supporting hyphal growth in the lung may allow identification of effective targets for treatment of fungal infections. During infection, *A. fumigatus* faces complex microenvironments in the human lung which include changes in deposition of nutrients, attack by immune cells, and decreases of the available oxygen content [3]. Indeed, it was reported that the mucus in the airways of cystic fibrosis patients, which can be colonised by *A. fumigatus* [2], was depleted of molecular oxygen [4]. Also, hypoxia was detected at the cellular level in murine models of invasive pulmonary aspergillosis by using the immunochemical hypoxia marker pimonidazole [5]. Thus, *A. fumigatus* encounters severe hypoxia when infecting a host and its ability to survive in this environment promotes its pathogenicity.

This article is protected by copyright. All rights reserved.

Accepted Article

The sterol-regulatory element binding protein SrbA mediates hypoxia responses in *A. fumigatus*. Its proteolytic activation is controlled by the intracellular concentration of sterols [6]. However, alternative regulatory mechanisms to adapt to hypoxia via mitochondrial ROS production have been suggested [7]. This indicates that in filamentous fungi, as shown in various human cells, moderate amounts of ROS can be essential signalling messengers that help cells to adapt to hypoxic or anoxic environments. Multiple studies in human cells suggested that ROS, produced by mitochondrial complex III of the respiratory chain, participate in stabilising the transcription factor hypoxia-inducible factor-1 (HIF-1) in response to oxygen depletion. Hypoxic ROS and nitric oxide (NO) introduce post-translational modifications into prolyl hydroxylases, which usually hydroxylate HIF-1 during normoxic conditions leading to proteasome-dependent degradation. These modifications change activities of prolyl hydroxylases including their interaction with HIF-1, and thus influence the expression of hypoxia-inducible genes [8, 9]. Likewise, it was shown that hypoxic ROS served as a cellular signal for adaptation to this environment in multicellular organisms and yeasts [9-11]. More than one decade ago, it was reported that *S. cerevisiae* exposed to anoxia faced transient oxidative stress, which possibly initiated the induction of hypoxic genes [10]. Similarly, redox-sensitive molecules may modulate hypoxia adaptation in filamentous fungi.

Overall, there is growing evidence that thiol-based redox switches are employed in eukaryotic cells to regulate the activity of proteins [12]. Classical shotgun proteomic workflows of determining protein levels cannot provide appropriate knowledge about proteins that are modified by hypoxia-induced ROS in *A. fumigatus*. However, application of redox proteomics allows identifying redox-sensitive molecules or, more precisely, the assessment of reversibly oxidised cysteines. Cysteine thiol groups (-SH) are highly reactive, and can be oxidised to sulphenic acid or disulphide bonds by ROS. S-nitrosylation by NO and S-glutathionylation

This article is protected by copyright. All rights reserved.

Accepted Article

by glutathione also represent frequent oxidative modifications of cysteine residues of proteins. The introduction of these modifications in target proteins may lead to changes in the protein structure and/or its function [13]. Therefore, the elucidation of redox-based changes in the *A. fumigatus* proteome under hypoxia may provide important information about proteins which are functionally altered by this condition.

In this study, we analysed the *A. fumigatus* redox proteome under hypoxia. After confirming increased amounts of ROS in the fungus grown in a severely hypoxic environment (0.2% O_2), we applied a redox proteomic approach to identify proteins, which undergo modifications by hypoxia-induced ROS. With this method, we found a set of proteins that was specifically oxidised when the molecular oxygen concentration dropped. This included several proteins that are important for maintaining redox balance and mitochondrial function. Especially noteworthy is a protein with reversibly oxidised cysteine residues in response to hypoxia (AFUA_3G09780), whose orthologues (Coa6) are important for mitochondrial respiratory complex IV assembly and copper homeostasis. Lack of this protein in *A. fumigatus* resulted in the complete abolishment of fungal growth under hypoxia, which confirmed the significance of complex IV during growth of *A. fumigatus* under oxygen-limiting conditions. To summarize, our work defined important cellular pathways that are either targets of hypoxia-induced ROS damage or may contribute to hypoxia adaptation. For this reason, they may be linked to fungal-specific fitness attributes and virulence determinants.

2. Material and methods

2.1. Fungal strains and growth conditions

A. fumigatus wild-type strains ATCC 46645, CEA10 (FGSC A1163; wild type in most experiments) and its derivative CEA17Δ*akuB*^{KU80} [14], the strain Afyap1 [15] expressing an Af*yap1*-

This article is protected by copyright. All rights reserved.

Accepted Article

eGFP fusion, ΔAf*yap1*, and Δ*coa6* (this study) were used. Fungal cultures were maintained at 37 °C on *Aspergillus* minimal medium (AMM) agar [16]. When required, 100 µg/ml hygromycin (Invivogen) was added. Conidia were harvested from agar plates using water and enumerated with a Thoma cell counting chamber.

2.2. Measurement of ROS production

A suspension of 10^4 conidia/ml in AMM [16] was dispensed into 96-well F-bottomed Microplates (Greiner) and incubated 16 h at 37 °C. Plates were placed into a hypoxic atmosphere, which consisted of 0.2% (v/v) O_2 and 5% (v/v) CO_2 (H35 Hypoxystation, Don Whitley Scientific, UK) at 37 °C. Fungal hyphae were stained with 3 µM 2',7'-dichlorofluorescein diacetate at 37 °C for 30 min directly in the hypoxic station. Two plates were left in the hypoxic station for 1 or 2 h. One plate was placed to the normoxic conditions for 1 h after being under hypoxia for 2 h. To remove the excess unreacted fluorescent probe, cells were washed with warm PBS. Before fluorescence measurement, plates stained in the hypoxic station were tightly closed with parafilm to avoid oxygen exposure. Fluorescence intensity was immediately measured with an excitation filter at 485 nm and an emission filter at 530 nm in a microtiter plate reader (Infinite 200 Pro, Tecan, Switzerland) at 37 °C. The experiment was repeated three times. For calculations, the fluorescence measured in the control mycelia of each replicate (cultivated under normoxic condition) was set to 100%. Fluorescence of each sample was expressed in percent of intensity of the corresponding control.

2.3. Microscopical analysis of AfYap1 localization under hypoxia

For fluorescence microscopy, 10^4 conidia of *A. fumigatus* AfYap1 strain in 500 µl AMM were inoculated into µ-Slide 4-well coverslip (ibidi) and cultivated for 16 h at 37 °C. Then, coverslips were transferred to the hypoxia workstation (0.2% [v/v] O_2 and 5% [v/v] CO_2).

This article is protected by copyright. All rights reserved.

Accepted Article

After 0.5, 1, and 2 h, hyphae were directly fixed with formaldehyde inside the hypoxia station. One sample was placed into the normoxic incubator for 1 h before fixation to examine AfYap1 localization after reoxygenation. Following subsequent nuclei staining with Hoechst 34580, AfYap1 cellular distribution was monitored by fluorescence microscopy with a Zeiss Axio Imager M2 (Zeiss, Germany).

2.4. Large-scale cultivation of *A. fumigatus* under oxygen-limiting conditions

The *A. fumigatus* wild-type strain CEA10 was grown at 37 °C in a fermenter as previously described [17]. Briefly, the cultivation was started by inoculation of 3×10^5 conidia/ml in AMM. Fermentation started as a batch culture for 20 h under aerobic conditions (21% [v/v] O_2 atmospheric pO_2). Then, the oxygen content of the culture was set to hypoxic conditions (0.2% [v/v] O_2 atmospheric pO_2) for 2 h. Subsequently, aerobic conditions were reestablished for 1 h. Fermentation parameters such as growth rate and glucose consumption were constantly monitored (Fig. S1B). In total, five samples were taken from the batch cultivation as shown in Fig. S1A. The harvested mycelium was frozen in liquid nitrogen and used for protein isolation.

2.5. Redox proteomics: Indirect labelling of oxidised cysteines

Protein extraction was performed by adding 300 µl lysis buffer containing 1% (w/v) SDS, 150 mM NaCl, 100 mM TEAB (Triethylammonium bicarbonate) (Sigma-Aldrich), 4 mM EDTA, and 1 tablet of cOmplete Ultra Protease Inhibitor Cocktail (Roche) to approximately 100 mg mycelia that had been ground under liquid nitrogen. The blocking reagent iodoacetamide (IAM) was added to the lysis buffer to a concentration of 100 mM immediately before usage. The cell lysate was sonicated in a water bath at 37 °C for 30 min. After 15 min centrifugation at 14,000 × *g*, the supernatant was collected and transferred to new tubes. Ex-

This article is protected by copyright. All rights reserved.

Accepted Article

cess iodoacetamide (IAM) was removed by methanol/chloroform protein precipitation [18]. Obtained pellets were solubilised in 100 µl of 100 mM TEAB with subsequent sonication in a water bath for 15 min and vortex mixing. The reduction buffer containing 0.5 M TCEP (tris(2-carboxyethyl)phosphine) (Calbiochem) in 100 mM TEAB was added and the samples were incubated at 55 °C for 1 h. Each 10 µl of iodoTMTsixplex isobaric label reagents (Thermo Fisher Scientific) dissolved in methanol were added to the samples as follows:

Reporter Ions	Biological Replicate 1	Biological Replicate 2	Biological Replicate 3
126	20 h normoxia	-	1 h reoxygenation
127	0.5 h hypoxia	20 h normoxia	-
128	1 h hypoxia	0.5 h hypoxia	20 h normoxia
129	2 h hypoxia	1 h hypoxia	0.5 h hypoxia
130	1 h reoxygenation	2h hypoxia	1 h hypoxia
131	-	1 h reoxygenation	2 h hypoxia

The reaction was performed at 37 °C in the dark for 60 min. 0.5 mM DTT was added to quench the reaction. All labelled samples corresponding to each biological replicate were pooled together on a 3 kDa centrifugal filter. Excess of iodoTMT was removed by centrifugation (15 min, 14,000 × *g*, 4 °C). After washing, proteins were recovered from the filters with 100 mM TEAB. Following trypsin digestion, peptides were lyophilised and suspended in 0.05% (v/v) TFA in H_2O/ACN 98/2. Before LC-MS/MS analysis, the peptides were desalted and concentrated with the help of C18 clean-up columns (Protea Biosciences, SP15096KIT) according to the manufacturer's protocol.

2.6. TMTsixplex labelling

Protein-containing samples, extracted as mentioned above, were also labelled with amino-reactive TMTsixplex isobaric label reagents (Thermo Fisher Scientific) to measure the relative abundance of proteins. Previously alkylated samples were reduced with TCEP and additionally alkylated with IAM. The labelling of three biological replicates of each time point

This article is protected by copyright. All rights reserved.

Accepted Article

with TMTsixplex was performed according to the manufacturer's instructions (see also Table S3).

2.7. LC-MS/MS analysis

LC-MS/MS analysis of samples labelled with iodoTMT$^{(1)}$ or TMT$^{(2)}$ was performed on an Ultimate 3000 nanoLC coupled to a QExactive Plus mass spectrometer (both Thermo Fisher Scientific, Waltham, MA, USA). By using an Acclaim PepMap column set (Thermo Fisher Scientific), peptides were trapped (2 cm x 75 µm, 3 µm) at 5µl/min (0.05% [v/v] TFA, 2% [v/v] ACN) and separated (50 cm × 75 µm, 2µm) at 300 nl/min and 40 °C using a binary gradient elution of eluents A (0.1% HCOOH) and B (0.1% HCOOH, 90% ACN): 0-4 min at 4%B, 90 min at 9%B, 130 min at 12.5%B, 180 min at 17%B, 200 min at 20%B, 220 min at 24%B, 250 min at 35%B, 260 min at 44%B, 265 min at 50%B, 270 min at 55%B, 275 min at 70%B, 280-290 min at 96%B, 291-360 min at 4%B.

Positively charged ions were generated at 2.2 kV spray voltage using a stainless steel emitter and a Nanospray Flex Ion Source. The mass spectrometry instrument was operated in Full MS / dd MS^2 (Top10) mode. Full scan precursor ion monitoring was performed at *m/z* 300-1600 amu, R=70k$^{(1)}$/140k$^{(2)}$ (FWHM), max. injection time of 120$^{(1)/}$100$^{(2)}$ ms, and an AGC (automatic gain control) target of 1e6$^{(1)}$/3e6$^{(2)}$. Data-dependent acquisition of up to 10 most abundant precursor ions per scan cycle with a charge state (z) of 2-6 were selected (isolation width of m/z 2.0$^{(1)}$ and 0.7$^{(2)}$ for HCD fragmentation at 36% NCE using nitrogen collision gas. Dynamic exclusion of precursor ions was set to 40 s. Fragment ions were monitored at R=17.5k (FWHM), max. injection time of 120$^{(1)}$/100$^{(2)}$ ms, and an AGC (automatic gain control) target of 2e5. The fixed first mass was set to m/z 100. The LC-MS/MS instrument was operated by Thermo/Dionex Chromeleon Xpress 6.8 and Xcalibur 3.0.63 software.

This article is protected by copyright. All rights reserved.

Accepted Article

2.8. Protein database search and iodoTMT and TMT reporter ion quantitation

Proteome Discoverer 1.4 (Thermo Fisher Scientific) was used to process mass spectrometry raw files. Tandem mass spectra were searched against *A. fumigatus* Af293 (27.09.2015, *Aspergillus* Genome Database, AspGD) using the algorithms of Mascot 2.4.1 (Matrix Science, UK), Sequest HT, and MS Amanda. Two missed cleavages were allowed for tryptic peptides. The precursor mass tolerance was set to 10 ppm and the fragment mass tolerance was set to 0.02 Da. For the iodoTMT analysis, dynamic modifications were oxidation of Met and carbamidomethylation or iodoTMTsixplex reaction of Cys residues. For TMTsixplex analysis, dynamic modifications were the carbamidomethylation of Cys by iodoacetamide and TMTsixplex at the ε-NH_2 group of Lys and the peptide N-terminus. Percolator node and a reverse decoy database were used to validate peptide spectral matches (PSMs). At least 2 peptides per protein and a strict target false discovery (FDR) rate < 1% were required for positive protein hits. Only unique peptides with an integration tolerance of 10 ppm using the most confident centroid were considered for iodoTMT quantification. Quan channel correction in accordance with the isotopic distribution was applied and the reporter ion ratios were normalized based on the protein median. The proteins were considered significantly modified (iodoTMT) or upregulated (TMT) when a fold change was greater than 1.5 in at least two biological replicates. In addition, normalisation to protein levels was performed. Accordingly, iodoTMT labelled proteins were assigned as differentially oxidised, only if their abundance, identified by TMT labelling, showed no change. The mass spectrometry data were uploaded to the ProteomeXchange Consortium via the PRIDE [19] partner repository with the dataset identifier PXD006822.

Annotated protein sequences were categorised using the Functional Catalogue (FunCat), which is implemented in the FungiFun2 web tool [20]. An enrichment analysis using hyperge-

This article is protected by copyright. All rights reserved.

Accepted Article

ometric distribution and a *p*-value threshold of >0.05 with all known categories of the proteome as reference was conducted.

2.9. Inhibition zone assay

Petri dishes with 10 mL AMM bottom-agar were covered with a layer of 10 mL top-agar containing 1×10^8 conidia. In the centre, 100 µL of 0.75 M TCEP (Calbiochem), 3% (v/v) H_2O_2, 0.1 M diamide (Sigma-Aldrich), or 2% (v/v) tert-butyl hydroperoxide (tBOOH) (Sigma-Aldrich) were filled in a hole of 10 mm diameter. Diameter of the inhibition zones was determined after 24 h of cultivation at 37 °C under normoxic or hypoxic conditions.

2.10. Determination of the cytochrome C oxidase activity

Activity of the cyctochrome C oxidase was measured as described in Spinazzi *et al*.[21]. *Aspergillus fumigatus* strains CEA17Δ*akuB* and Δ*coa6* were cultivated in triplicate in *Aspergillus* minimal medium (AMM) until an equal concentration of remaining glucose could be measured (24 and 48 h, respectively). Harvested mycelium was ground under liquid nitrogen and proteins were extracted in PBS containing cOmplete protease inhibitor cocktail (Roche). The decrease of reduced cytochrome C (from equine heart, Sigma-Aldrich) was monitored for 5 min. at 550 nm with an UV mini 1240 spectrophotometer (Shimadzu). Cytochrome C oxidase activity was specifically inhibited by the addition of 0.5 or 1 mM KCN.

2.11. Generation of the Δ*coa6* deletion mutant

A. fumigatus CEA17Δ$akuB^{KU80}$ [14] was used as a parental strain to obtain the Δ*coa6* deletion strain by homologous recombination following the transformation of protoplasts [22]. For deletion of *coa6* (AFUA_3G09780), the flanking regions were amplified from genomic DNA with the primer pairs P1 and P3, and P4 and P6 as indicated in the Table S1. PCR was con-

This article is protected by copyright. All rights reserved.

Accepted Article

ducted with Phusion Flash High-Fidelity polymerase (ThermoFisher, F548S). By this reaction, overlapping ends to the hygromycin resistance cassette were introduced at the 3'-end of the upstream flanking region and at the 5'-end of the downstream flanking region of the genes. The hygromycin resistance cassette was amplified from plasmid pUChph [23] using primers 1_hph and 2_hph (Tab. S1). The *coa6* deletion construct was obtained by a fusion PCR using primers P2 and P5. The generated mutants were verified by Southern blot (Fig. S2) as described in [24]. The gene specific DNA probe was generated by PCR using the primers P1 and P3. Genomic DNA, isolated from the wild type and the mutant, was digested with the restriction enzyme *Kpn*I (NEB, R0142).

This article is protected by copyright. All rights reserved.

Accepted Article

3. Results and Discussion

3.1 Hypoxia-induced ROS formation in A. fumigatus

Redox regulation of hypoxia signalling has not yet been investigated in filamentous fungi. In this study, we demonstrated increased intracellular accumulation of ROS in *A. fumigatus* during hypoxic cultivation. Although counterintuitive at first, studies in yeast have indicated that respiratory complex III is a significant producer of ROS during hypoxia [7, 9]. As depicted in Fig. 1, fluorescence captured from the oxidation of the probe 2',7'-dichlorodihydrofluorescein to the highly fluorescent 2',7'-dichlorofluorescein by intracellular ROS, was increased in hypoxic mycelia of *A. fumigatus* in contrast to mycelia cultivated under normoxic conditions. The amount of accumulated ROS remained high after 2 h of hypoxia cultivation and reoxygenation. Based on this observation, we further analysed the physiological role of hypoxia-induced ROS in *A. fumigatus*.

To avoid oxidative damage, the generation of hypoxic ROS needs to be tightly regulated and controlled. This is reflected in the transcriptomic data of the hypoxic response of *A. fumigatus*; transcript levels of various antioxidative enzymes were affected by low oxygen levels. In particular, different catalase genes were upregulated in response to short-term as well as long-term hypoxia (reviewed in Hillmann *et al.* [25]). Here, an inhibition zone assay with strong oxidizing agents was performed to evaluate the importance of catalases for *A. fumigatus* under low oxygen conditions. The fungal growth was more strongly inhibited by a suicide substrate for catalases, tert-butyl hydroperoxide (tBOOH), under hypoxia than under normoxia (Fig. 2A). This result suggests that inhibition of catalases by tBOOH [26] may influence the adaptation of *A. fumigatus* to hypoxia. In contrast to tBOOH, the diameter of the inhibition zone in the presence of H_2O_2 appeared to be the same under both conditions. How-

This article is protected by copyright. All rights reserved.

Accepted Article

ever, growth of the ΔAf*yap1* strain, which lacks the major oxidative stress regulator AfYap1 [27], was comparably more affected by H_2O_2 during oxygen deprivation (Fig. 2B). This finding suggests a possible involvement of this transcription factor in the cellular response to H_2O_2 in low oxygen environments. However, the combination of two stresses, hypoxia and strong oxidative stress, may exert non-additive effects upon the ROS-sensitive strain ΔAf*yap1*in terms of growth inhibition. All in all, catalases and other antioxidative enzymes may contribute to maintaining the redox balance during the hypoxic growth of *A. fumigatus*.

Serving as signalling molecules, hypoxia-induced ROS may have an impact on the gene expression level of the transcription factor AfYap1 that regulates the fungal oxidative stress response. Indeed, *Afyap1* gene expression was increased after 2 h of exposure to hypoxic conditions [28]. To show the activation of Afyap1 under hypoxia, we monitored the cellular distribution of the AfYap1_GFP fusion protein in the *A. fumigatus* strain Afyap1 during the switch from normoxia to hypoxia. As shown in Fig. 3, the transcription factor AfYap1 accumulated in the nucleus under hypoxia. Interestingly, after reoxygenation, the AfYap1_GFP fluorescence was mainly detected in the cytosol. This may imply that gene regulation by AfYap1 contributes to hypoxic growth. Consistently, the proposed AfYap1 target genes Afu3g00730 and Afu5g14680 [27] showed increased protein levels under hypoxia (Table S3). However, deletion of this transcription factor did not change the ability of *A. fumigatus* to adapt to hypoxia (data not shown). One can speculate that either the hypoxia-induced ROS levels do not have significant adverse effects on the growth of *A. fumigatus* or other regulators of oxidative stress resistance, such as Skn7 or AtfA may be activated under hypoxia to compensate for the absence of AfYap1 [29]. It should be noted that little is known about the role of Yap1 in fungi under hypoxic conditions. Bourdineaud *et al.* [30] reported about the activation of the cell wall mannoprotein Tir1 of *S. cerevisiae* by Yap1 at low oxygen levels.

This article is protected by copyright. All rights reserved.

Accepted Article

However, an orthologue of Tir1 does not exist in the genome of *A. fumigatus*. In general, Yap1 seems to act not only as an important regulator of the antioxidative stress response, but also as a regulator of several other pathways including carbon utilisation and asexual sporulation as shown in *A. nidulans* [31].

3.2 Reversible protein thiol oxidation in A. fumigatus during hypoxia

To investigate putative targets of hypoxic ROS, we examined the protein oxidative modifications in *A. fumigatus* cultured in low oxygen. A batch cultivation of *A. fumigatus* in a fermenter system with defined oxygen partial pressures was carried out. Overall 3291 proteins were identified by proteomic analysis (all proteins) of *A. fumigatus* mycelia cultivated in the hypoxic fermenter (Tab. S2). Only a minority was labelled with the sulfhydryl (-SH) reactive isobaric tag iodoTMT, consistent with a low occurrence of oxidised cysteines in proteins. The highest number (n=18) of oxidised proteins was detected after 1 h of hypoxic cultivation (Tab. 1, Tab. S2). Intriguingly, after reoxygenation, the quantity of oxidised cysteines decreased. At that time point, only 9 proteins showed higher oxidation compared to proteins under control condition. In preliminary tests (data not shown) the efficiency of iodoTMT-labelling of cysteines was 99.6 (±0.1).

In order to normalise obtained redox proteomic data, changes in protein abundance were quantified by labelling the extracted proteins with TMT reagents. The majority of proteins identified by redox proteomics showed no significant alteration in abundance (Tab. S3), confirming that changes identified by redox proteomics happened due to alterations in cysteine oxidation but not protein abundance. Even though the changes in protein levels were primarily determined to normalize redox proteomics data, we present the analysis of proteins, which were differentially regulated in *A. fumigatus* during hypoxia (Tab. 2, Fig. S3). 183 proteins showed changes in abundance above ±1.5-fold. The proteome changed more drastically at

This article is protected by copyright. All rights reserved.

Accepted Article

later time points (2 h) of hypoxia (124 over-, 20 underrepresented proteins) or after reoxygenation (74 over- and 11 underrepresented proteins) than at earlier time points of hypoxia (12 over- and 5 underrepresented proteins after 0.5 h of hypoxia and 40 over- and 19 underrepresented proteins after 1 h of hypoxia). Protein set enrichment analysis using Functional Catalogue (FunCat) annotations revealed that proteins involved in respiration/electron transport, glycolysis/gluconeogenesis, the TCA-cycle, and ubiquinone metabolism increased during the course of the experiment (Fig. S3). After 1 h of reoxygenation, the categories amino acid, nitrogen/sulphur, and C-2 compound metabolism as well as alcohol fermentation also increased (Fig. S3). Only six proteins showed significantly altered levels at all time points, while the abundance of six further proteins significantly changed throughout the period of hypoxia (Fig. S3). Previously, it was shown that the levels of some of these proteins, like the NO-detoxifying flavohemoprotein FhpA (AFUA_4G03410) were increased in *A. fumigatus* grown under low oxygen conditions [17, 32]. However, the alcohol dehydrogenase AlcC (AFUA_5G06240), the fungoglobin FglA, the hypoxia transcriptional regulator SrbB, and the alternative oxidase AoxA (AFUA_2G05060) have been reported as highly upregulated during hypoxia only in transcriptomic analyses so far [17, 33]. The latter, AoxA, showed also increased activity in an oxygen consumption assay in *A. fumigatus* grown in hypoxic conditions [5]. It has been shown that AoxA plays a critical role in limiting mitochondrial ROS formation [34], and thus contributes to the maintenance of the cellular redox balance in mitochondria at low oxygen levels.

Therefore, current proteomic analysis can support previous proteomic and transcriptomic data as well as reveal new proteins with high abundance in *A. fumigatus* exposed to hypoxia. For example, we found that the synthesis of a mitochondrial proline oxidase (AFUA_6G08760) and a urate oxidase (AFUA_2G10520) was increased after 1 h of hypoxia. Considering re-

This article is protected by copyright. All rights reserved.

Accepted Article

ports about involvement of these proteins in cellular redox signalling and regulation of cellular respiration in higher eukaryotes, we can speculate that the activity of these enzymes in hypoxic fungal cells contributes to the production of ROS and a subsequent redox signalling cascade [35]. However, this possibility requires further investigation.

Proteins with putative roles in carbohydrate metabolism, respiration, protein folding, redox homeostasis, and amino acid synthesis were mainly found to be more oxidised under hypoxia (Tab. 1). Some of these cellular processes were reported to be regulated in response to hypoxia. For instance, it was shown that the structure of the cell wall can be altered during hypoxic growth of *A. fumigatus* [36]. In line, we detected a protein annotated as AFUA_5G02740 to be exclusively oxidised when oxygen levels dropped. This protein is an alpha-1,2-mannosyltransferase that is involved in the biosynthesis of the structurally important cell wall polymer galactomannan [37]. This finding supports the idea that the cell wall of *A. fumigatus* undergoes changes in response to oxygen limitation and that these changes may occur due to redox modifications in key enzymes.

Interestingly, the Cu/Zn superoxide dismutase Sod1 (AFUA_5G09240) showed increased oxidative modification of a cysteine residue (Fig. S4A) after 1 h of hypoxic exposure, whereas after 2 h of hypoxia and reoxygenation the oxidative status of this protein was not significantly different from a control under normoxia (Tab. 1). It is most likely that high amounts of generated hypoxic ROS altered Sod1 properties at the initial step of hypoxic adaptation. In *S. cerevisiae*, it was shown that the disulphide bond between Cys58 and Cys147 stabilizes the structure of yeast SOD1 and regulates its enzymatic activity [38]. Molecular oxygen is necessary to induce disulphide formation in yeast SOD1. A recent quantitative redox proteomics study in yeast showed that the respective cysteines are oxidised to around 70% *in vivo*. The authors assumed that only newly synthesised enzymes and those in transit to the intermem-

This article is protected by copyright. All rights reserved.

Accepted Article

brane space of mitochondria have reduced cysteines [39]. Our study suggests that the level of oxidative modifications increases when oxygen supply drops and ROS levels may increase in parallel.

Another protein involved in maintaining redox homeostasis, a putative thioredoxin 1 (Trx1) (AFUA_5G11320), was oxidised under hypoxia as well (Tab. 1). Importantly, cysteine residues Cys34 and Cys37 that are part of the conserved, redox CXXC motif reflected higher oxidation after 1 and 2 h of hypoxia as well as reoxygenation than under control conditions (Tab. 1, Fig. S4B). The reduction of oxidised proteins by thioredoxins is performed through the conserved CXXC motif via reversible disulphide formation [40]. Hence, oxidation of *A. fumigatus* Trx1 under hypoxia possibly occurred due to oxidoreductase activity of the enzyme, which acted to reduce the oxidised cysteine residues of target proteins. Interestingly, also the non-conserved Cys29 underwent thiol modifications that may also have regulatory functions.

Our redox proteomic study also revealed an altered oxidation status of essential enzymes for the protein folding machinery in the endoplasmic reticulum (ER). Protein disulphide isomerase PdiA (AFUA_2G06150) showed increased oxidative thiol modifications under hypoxia in comparison to normoxia. It is well known that homologs of PdiA are redox regulated [41]. Hypoxic thiol modifications in the *A. fumigatus* PdiA were found on conserved cysteines (Fig. S4C). These cysteines do not belong to the important thioredoxin-like domain CXXC that defines enzymatic properties of PdiA [42]. In contrast, it was found that these cysteine residues are part of a non-active site of PdiA. However, the formation of a structural disulphide in the non-active site of PdiA facilitates the oxidase activity of N-terminally located redox-active cysteines of the PdiA [43].

This article is protected by copyright. All rights reserved.

Accepted Article

To gain more insights into the role of proper protein folding in *A. fumigatus* under hypoxia we tested the inhibitory activity of diamide under low oxygen levels. Diamide causes depletion of the intracellular glutathione pool and therefore increases the formation of protein disulphide bridges [44]. In addition, previous analysis of the transcriptional response of *S. cerevisiae* revealed that diamide caused disruption of proper disulphide isomerisation in the ER [45]. Accordingly, *A. fumigatus* displayed slightly higher sensitivity to diamide under hypoxia compared to normoxia (Fig. S5). In addition, we showed that in the presence of TCEP, which reduced protein disulphide bridges, the growth of *A. fumigatus* was more strongly inhibited under oxygen deprivation (Fig. S5). We thus can conclude that the maintenance of redox homeostasis and proper ER folding activity are of importance under low oxygen conditions.

3.3 The role of the cytochrome oxidase assembly factor 6 (Coa6) during hypoxic growth

It was most intriguinginig that the indirect labeling of oxidised cysteines identified a homologue of *S. cerevisiae* COA6. In *A. fumigatus* annotated as AFUA_3G09780, it was more oxidised under hypoxia in comparison to its redox state under normoxia (Tab. 1). Many studies have indicated that *S. cerevisiae* COA6 is important for the assembly of mitochondrial complex IV in the respiratory chain, in particular the copper-containing subunit COX2 [46-48]. Moreover, the importance of cysteine residues of the conserved Cx9CxnCx10C motif in COA6 was well-established showing that each cysteine belonging to the motif was essential for the function of the protein [46]. Also, it was suggested that an optimal modification of COA6 (possibly, when two cysteines are oxidised and two others are reduced) was required for its function [48]. However, the cysteine residues that form a disulphide bond in COA6 have not been defined yet. Our redox proteomic analysis suggests that the two oxidised cysteines forming a disulphide bridge are crucial for a proper function of the protein (Fig. 4A).

This article is protected by copyright. All rights reserved.

Accepted Article

To evaluate the importance of Coa6 in *A. fumigatus*, the gene encoding this protein was deleted. Interestingly, the obtained knockout showed absolutely no growth when grown on different media in the hypoxic chamber (Fig. 4B). Considering that homologs of *A. fumigatus* Coa6 are involved in binding and delivery of copper to complex IV [46], we hypothesized that the lack of *coa6* led to an accumulation of unbound copper in *A. fumigatus*. This hypothesis was confirmed by the fact that the addition of the copper chelator BCS could improve the growth of the parent strain (CEA17Δ*akuB*) at 0.2 % O_2, while the growth of Δ*coa6* did not improve growth under hypoxia (Fig. 4C). In line, the copper-binding metallothionein CmtA, which is most probably involved in maintaining copper homeostasis [49], showed increased protein levels during the whole course of hypoxic growth (Table 2). Thus, the deletion of the *coa6* gene may cause both a reduced activity of mitochondrial complex IV and an increased, toxic level of copper. To support this conclusion, we determined the cytochrome C oxidase activity (complex IV) in protein extracts of the parent strain CEA17Δ*akuB* and Δ*coa6* mutant strain. The enzymatic activity was 17.4 (±2.6) nmol·cytochrome C min^{-1}·mg^{-1} protein in strain CEA17Δ*akuB*, while it was 20-fold lower in the *Δcoa6* mutant strain with 0.84 (±0.24) nmol·cytochrome C min^{-1}·mg^{-1} protein. To check the specificity of the complex IV activity, we added 0.5-1 mM KCN to the assay, which resulted in a complete abolishment of cytochrome C oxidase activity.

This demonstrates that deletion of the *coa6* gene abolished hypoxic growth of *A. fumigatus* due to dysfunctional complex IV and not due to copper toxicity, because binding of potentially toxic excess copper did not rescue the growth of the mutant in low oxygen environments (Fig. 4C).

4. Concluding remarks

This article is protected by copyright. All rights reserved.

Accepted Article

In a previous phenotypic characterisation, it was revealed that *A. fumigatus* was especially sensitive to inhibitors of complex IV when grown under oxygen deprivation [50]. Furthermore, hypoxia was shown to increase the abundance of several components of the respiratory chain complex IV [32]. Until now, the contributors to the maintenance of the complex IV activity under hypoxia remained unknown. Considering that the deletion of the gene encoding Coa6 resulted in complete abrogation of *A. fumigatus* hypoxic growth (Fig. 4B, C), we can conclude that redox proteomics helped us to reveal Coa6 as an essential factor of respiration under hypoxia in *A. fumigatus*.

Acknowledgement

We thank Silke Steinbach, Till Kindel, and Michael Cyrulies for their excellent technical assistance. Work of T.K., O.K. and A.A.B was supported by the Deutsche Forschungsgemeinschaft within the Collaborative Research Center TR124 FungiNet (project A1 and Z2). The work of E.S. was supported by the International Leibniz Research School for Microbial and Biomolecular Interactions (ILRS) and by the Medical Research Council Centre for Medical Mycology at the University of Aberdeen (MR/N006364/1). We thank Matthew Blango and Falk Hillmann for the critical reading of the manuscript.

Supporting Information

Supporting information is available from the Wiley Online Library or from the author.

Conflict of interest

The authors have declared no conflict of interest.

5. References

This article is protected by copyright. All rights reserved.

Accepted Article

[1] J. P. Latge, Clin Microbiol Rev 1999, 12, 310.

[2] J. King, S. F. Brunel, A. Warris, J Infect 2016, 72 Suppl, S50.

[3] T. Hartmann, C. Sasse, A. Schedler, M. Hasenberg, M. Gunzer, S. Krappmann, Int J Med Microbiol 2011, 301, 408.

[4] D. Worlitzsch, R. Tarran, M. Ulrich, U. Schwab, A. Cekici, K. C. Meyer, P. Birrer, G. Bellon, J. Berger, T. Weiss, K. Botzenhart, J. R. Yankaskas, S. Randell, R. C. Boucher, G. Döring, J Clin Invest 2002, 109, 317.

[5] N. Grahl, S. Puttikamonkul, J. M. Macdonald, M. P. Gamcsik, L. Y. Ngo, T. M. Hohl, R. A. Cramer, PLoS Pathog 2011, 7, e1002145.

[6] S. D. Willger, S. Puttikamonkul, K. H. Kim, J. B. Burritt, N. Grahl, L. J. Metzler, R. Barbuch, M. Bard, C. B. Lawrence, R. A. Cramer, Jr., PLoS Pathog 2008, 4, e1000200.

[7] R. D. Guzy, M. M. Mack, P. T. Schumacker, Antioxid Redox Signal 2007, 9, 1317.

[8] K. D. Mansfield, R. D. Guzy, Y. Pan, R. M. Young, T. P. Cash, P. T. Schumacker, M. C. Simon, Cell Metab 2005, 1, 393.

[9] R. D. Guzy, B. Hoyos, E. Robin, H. Chen, L. Liu, K. D. Mansfield, M. C. Simon, U. Hammerling, P. T. Schumacker, Cell Metab 2005, 1, 401.

[10] R. Dirmeier, K. M. O'Brien, M. Engle, A. Dodd, E. Spears, R. O. Poyton, Journal of Biological Chemistry 2002, 277, 34773.

[11] G. B. Waypa, J. D. Marks, M. M. Mack, C. Boriboun, P. T. Mungai, P. T. Schumacker, Circ Res 2002, 91, 719.

[12] N. Brandes, S. Schmitt, U. Jakob, Antioxid Redox Signal 2009, 11, 997.

[13] K. M. Holmstrom, T. Finkel, Nat Rev Mol Cell Biol 2014, 15, 411.

[14] M. E. da Silva Ferreira, M. R. Kress, M. Savoldi, M. H. Goldman, A. Hartl, T. Heinekamp, A. A. Brakhage, G. H. Goldman, Eukaryot Cell 2006, 5, 207.

This article is protected by copyright. All rights reserved.

Accepted Article

[15] E. Shekhova, O. Kniemeyer, A. A. Brakhage, Antimicrob Agents Chemother 2017, 61, e00978.

[16] K. T. Bergh, O. Litzka, A. A. Brakhage, J Bacteriol 1996, 178, 3908.

[17] B. M. Barker, K. Kroll, M. Vödisch, A. Mazurie, O. Kniemeyer, R. A. Cramer, BMC Genomics 2012, 13, 62.

[18] D. Wessel, U. I. Flugge, Anal Biochem 1984, 138, 141.

[19] J. A. Vizcaíno, A. Csordas, N. del-Toro, J. A. Dianes, J. Griss, I. Lavidas, G. Mayer, Y. Perez-Riverol, F. Reisinger, T. Ternent, Q. W. Xu, R. Wang, H. Hermjakob, Nucleic Acids Res 2016, 44, D447.

[20] S. Priebe, C. Kreisel, F. Horn, R. Guthke, J. Linde, Bioinformatics 2015, 31, 445.

[21] M. Spinazzi, A. Casarin, V. Pertegato, L. Salviati, C. Angelini, Nature protocols 2012, 7, 1235.

[22] G. Weidner, C. d'Enfert, A. Koch, P. C. Mol, A. A. Brakhage, Curr Genet 1998, 33, 378.

[23] B. Liebmann, M. Muller, A. Braun, A. A. Brakhage, Infect Immun 2004, 72, 5193.

[24] K. Kroll, E. Shekhova, D. J. Mattern, A. Thywissen, I. D. Jacobsen, M. Strassburger, T. Heinekamp, E. Shelest, A. A. Brakhage, O. Kniemeyer, Mol Microbiol 2016, 101, 92.

[25] F. Hillmann, E. Shekhova, O. Kniemeyer, Curr Genet 2015, 61, 441.

[26] H. Pichorner, G. Jessner, R. Ebermann, Arch Biochem Biophys 1993, 300, 258.

[27] F. Lessing, O. Kniemeyer, I. Wozniok, J. Loeffler, O. Kurzai, A. Haertl, A. A. Brakhage, Eukaryot Cell 2007, 6, 2290.

[28] L. Losada, B. M. Barker, S. Pakala, S. Pakala, V. Joardar, N. Zafar, S. Mounaud, N. Fedorova, W. C. Nierman, R. A. Cramer, Mycopathologia 2014, 178, 331.

This article is protected by copyright. All rights reserved.

Accepted Article

[29] D. Hagiwara, S. Suzuki, K. Kamei, T. Gonoi, S. Kawamoto, Fungal genetics and biology : FG & B 2014, 73, 138; C. Lamarre, O. Ibrahim-Granet, C. Du, R. Calderone, J. P. Latge, Fungal genetics and biology : FG & B 2007, 44, 682.

[30] J. P. Bourdineaud, G. De Sampaio, G. J. Lauquin, Mol Microbiol 2000, 38, 879.

[31] A. E. Mendoza-Martinez, F. Lara-Rojas, O. Sanchez, J. Aguirre, Frontiers in microbiology 2017, 8, 516.

[32] M. Vodisch, K. Scherlach, R. Winkler, C. Hertweck, H. P. Braun, M. Roth, H. Haas, E. R. Werner, A. A. Brakhage, O. Kniemeyer, J Proteome Res 2011, 10, 2508.

[33] F. Hillmann, J. Linde, N. Beckmann, M. Cyrulies, M. Strassburger, T. Heinekamp, H. Haas, R. Guthke, O. Kniemeyer, A. A. Brakhage, Mol Microbiol 2014, 93, 539.

[34] T. Magnani, F. M. Soriani, V. P. Martins, A. M. Nascimento, V. G. Tudella, C. Curti, S. A. Uyemura, FEMS microbiology letters 2007, 271, 230.

[35] L. Gabison, T. Prange, N. Colloc'h, M. El Hajji, B. Castro, M. Chiadmi, BMC Struct Biol 2008, 8, 32; J. Pandhare, S. Dash, B. Jones, F. Villalta, C. Dash, J Biol Chem 2015, 290, 25439; C. N. Hancock, W. Liu, W. G. Alvord, J. M. Phang, Amino acids 2016, 48, 859.

[36] K. M. Shepardson, L. Y. Ngo, V. Aimanianda, J. P. Latge, B. M. Barker, S. J. Blosser, Y. Iwakura, T. M. Hohl, R. A. Cramer, Microbes Infect 2013, 15, 259.

[37] T. Onoue, Y. Tanaka, D. Hagiwara, K. Ekino, A. Watanabe, K. Ohta, K. Kamei, N. Shibata, M. Goto, T. Oka, Scientific reports 2018, 8, 16918.

[38] Y. Furukawa, A. S. Torres, T. V. O'Halloran, Embo j 2004, 23, 2872.

[39] N. Brandes, D. Reichmann, H. Tienson, L. I. Leichert, U. Jakob, J Biol Chem 2011, 286, 41893.

[40] A. Holmgren, J Biol Chem 1989, 264, 13963; N. Nagarajan, S. Oka, J. Sadoshima, Free Radic Biol Med 2016.

[41] F. Hatahet, L. W. Ruddock, Antioxid Redox Signal 2009, 11, 2807.

This article is protected by copyright. All rights reserved.

Accepted Article

[42] B. Wilkinson, H. F. Gilbert, Biochim Biophys Acta 2004, 1699, 35.

[43] B. Wilkinson, R. Xiao, H. F. Gilbert, J Biol Chem 2005, 280, 11483.

[44] N. S. Kosower, E. M. Kosower, Methods Enzymol 1995, 251, 123.

[45] G. W. Thorpe, C. S. Fong, N. Alic, V. J. Higgins, I. W. Dawes, Proc Natl Acad Sci U S A 2004, 101, 6564.

[46] A. Ghosh, P. P. Trivedi, S. A. Timbalia, A. T. Griffin, J. J. Rahn, S. S. Chan, V. M. Gohil, Hum Mol Genet 2014, 23, 3596.

[47] D. Pacheu-Grau, B. Bareth, J. Dudek, L. Juris, F. N. Vogtle, M. Wissel, S. C. Leary, S. Dennerlein, P. Rehling, M. Deckers, Cell Metab 2015, 21, 823.

[48] D. A. Stroud, M. J. Maher, C. Lindau, F. N. Vogtle, A. E. Frazier, E. Surgenor, H. Mountford, A. P. Singh, M. Bonas, S. Oeljeklaus, B. Warscheid, C. Meisinger, D. R. Thorburn, M. T. Ryan, Hum Mol Genet 2015, 24, 5404.

[49] P. Wiemann, A. Perevitsky, F. Y. Lim, Y. Shadkchan, B. P. Knox, J. A. Landero Figueora, T. Choera, M. Niu, A. J. Steinberger, M. Wuthrich, R. A. Idol, B. S. Klein, M. C. Dinauer, A. Huttenlocher, N. Osherov, N. P. Keller, Cell Rep 2017, 19, 1008.

[50] K. Kroll, V. Pahtz, F. Hillmann, Y. Vaknin, W. Schmidt-Heck, M. Roth, I. D. Jacobsen, N. Osherov, A. A. Brakhage, O. Kniemeyer, Eukaryot Cell 2014, 13, 1241.

Figure legends

Figure 1. Comparative analysis of ROS accumulation in *A. fumigatus* under hypoxic and normoxic conditions. Determination of ROS: fungal mycelia were incubated under hypoxia for the indicated periods. Mycelia were stained with the oxidant-sensing probe 2',7'-dichlorofluorescin diacetate. Measurements were performed at 37 °C. For comparison, *A. fumigatus* was incubated under normoxic conditions for the indicated time periods; the determined fluorescence signal was set to 100%. Fluorescence of each sample was expressed in percent of intensity in comparison to the control. Welch Two sample t-test was used for significance testing of two groups. The bar graph represents mean ± SEM of four experiments. $p \leq 0.05$ and $p \leq 0.01$ were labelled with one and two asterisks, respectively.

This article is protected by copyright. All rights reserved.

Accepted Article

Figure 2. Phenotypic characterization of *A. fumigatus* with oxidizing agents under hypoxia compared to normoxia. A) Sensitivity of *A. fumigatus* wild type CEA10 against tBOOH and H_2O_2. The inhibition zones in a plate diffusion assay were measured 16 h after addition of the oxidizing agents. Welch Two sample t-test was used for significance testing of two groups. The bar graph represents mean ± SEM of three experiments. $p \leq 0.05$ was labelled with one asterisk. B) Sensitivity of ΔAf*yap1* and a corresponding wild-type strain ATCC_46645 to H_2O_2 under hypoxia. Representative pictures of the inhibition zone assays performed with the wild type and the ΔAf*yap1* mutant under hypoxic and normoxic conditions are shown. Lines represent the inhibition zones and areas outside of the lines indicate *A. fumigatus* growth.

Figure 3. AfYap1 accumulates in the nucleus when *A. fumigatus* mycelia are transferred to hypoxia (0.2% [v/v] O_2). Microscopic images of the *A. fumigatus* AfYap1_eGFP strain. 10^4 spores of the strain Af*yap1*_eGFP were cultivated in AMM for 16 h at 37 °C. Mycelia were shifted to hypoxia for the indicated time before fixation. Hoechst 34580 stained nuclei are shown in blue.

Figure 4. Coa6 sequence alignment and the phenotype of the Δ*coa6* deletion mutant. A) Coa6 sequence alignment. Coa6 sequences from *A. fumigatus*, *S. cerevisiae*, and *Homo sapiens* were aligned in T-coffee (www.ch.embnet.org/software/TCoffee.html) and color-coded using BOXSHADE. Identical sequences are shown with white text and highlighted in black. Conservative amino acids substitutions are shown with white text and highlighted in grey. Oxidised cysteines are indicated with arrows. Cysteines of the conserved Cx9CxnCx10C motif are highlighted in a blue rectangle. B) Droplet growth assay of Δ*coa6*. 5 µl aliquots of wild type (CEA17Δ*akuB*^{KU80}) and Δ*coa6* were spotted in a serial 10-fold dilution to reach final concentrations of 10^5, 10^4, 10^3, and 10^2 conidia on AMM agar plates or 1% peptone agar plates. Growth differences were detected after 48 h of incubation at 37 °C under normoxic or hypoxic atmospheres. C) Cultivation of the wild type and the Δ*coa6* strain in the presence of a copper chelator. 10^8 conidia of each strain were incubated in AMM with shaking (200 rpm) at 37 °C. Where indicated, bathocuproinedisulfonic acid (BCS) was added at a final concentration of 1 mM. Welch Two sample t-test was used for significance testing of two groups. The bar graph represents mean ± SEM of three experiments. $p \leq 0.05$ was labelled with one asterisk.

This article is protected by copyright. All rights reserved.

Accepted Article

Table 1. Differentially oxidised proteins in *A. fumigatus* during hypoxic cultivation (NS=not significant)

Locus Number	#Cys	M_r, kDa	Putative function	iodoTMT fold changes of oxidised protein			
				0.5 h hypox/ 20h norm	1 h hypox/ 20h norm	2 h hypox/ 20h norm	1 h reoxyg/ 20h norm
			Respiration / mitochondrial function				
AFUA_4G11390	6	17.9	Ubiquinol-cytochrome c reductase complex 17 kd protein	1.61	3.32	7.73	1.9
AFUA_6G02260	2	23.1	Mitochondrial membrane organization protein	NS	2.22	NS	NS
AFUA_3G09780	4	13.3	Mitochondrial respiratory chain complex IV assembly	NS	1.6	1.57	NS
AFUA_2G13010	4	10.9	Putative cytochrome c oxidase polypeptide	NS	1.6	1.59	NS
AFUA_3G08380	5	43.6	Inorganic diphosphatase	1.7	0.49	0.46	NS
AFUA_1G02620	4	18	Cytochrome C oxidase assembly mitochondrial protein	NS	NS	1.61	NS
			Carbohydrate metabolism				
AFUA_1G04620	10	37.9	Zinc-containing alcohol dehydrogenase	NS	1.86	NS	NS
AFUA_2G14750	8	35.6	Endo-arabinase	NS	1.64	1.52	1.51
AFUA_7G06140	7	78.4	1,4-beta-D-glucan glucanhydrolase	NS	1.55	NS	NS
AFUA_2G05910	8	54.2	Hexokinase	1.76	NS	NS	NS
			Protein folding / transport				
AFUA_2G06150	6	56.2	Protein disulfide isomerase	1.95	2.93	2.6	1.79
AFUA_2G03870	2	14.6	FK506-binding protein peptidyl-prolyl cis-trans isomerase	NS	1.6	NS	1.55
AFUA_1G04470	4	10.2	Protein transport	NS	NS	1.59	NS
			Redox homeostasis				
AFUA_5G11320	3	12	Allergen Asp f 29, putative thioredoxin	NS	2.31	2.23	1.59
AFUA_5G09240	2	16	Cu/Zn superoxide dismutase	NS	1.58	NS	NS
AFUA_4G05915	4	23.2	Thioredoxin peroxidase	NS	1.5	NS	NS
			Amino acid / protein synthesis				
AFUA_2G15590	10	167.5	Sulphite reductase	NS	1.73	1.54	NS
AFUA_2G10500	2	16	40S ribosomal protein Rps16	NS	NS	NS	1.698
			Cell wall maintenance				
AFUA_5G02740	10	46.5	Alpha-1,2-mannosyltransferase	NS	1.82	1.85	NS
AFUA_5G09580	8	15.6	Conidial hydrophobin RodA	NS	1.52	NS	NS
			Sterol transport				
AFUA_2G11340	8	27.3	Intracellular sterol transport	NS	1.6	1.73	NS
			Toxicity				
AFUA_5G02330	4	19.6	Allergen Asp f 1, ribonuclease mitogillin family of cytotoxins	NS	NS	NS	2.16
			Unknown				
AFUA_4G01290	6	25.2	Glycosyl hydrolase family 75 chitosanase	NS	NS	2.25	2.51
AFUA_8G00710	6	10.6	Unknown/putative secreted antimicrobial peptide	NS	1.58	2.56	4.28

This article is protected by copyright. All rights reserved.

Accepted Article

Table 2. Selected differentially abundant proteins in *A. fumigatus* during hypoxic cultivation (NS=not significant)

Locus Number	Putative function	TMT fold changes of protein abundance			
		0.5 h hypox/ 20h norm	1 h hypox/ 20h norm	2 h hypox/ 20h norm	1 h reox-yg/ 20h norm
	Respiration / mitochondrial function				
AFUA_2G05060	Alternative oxidase AoxA	2.70	2.71	4.33	3.26
AFUA_4G06790	Ubiquinol-cytochrome c reductase complex 14 kDa protein	NS	NS	3.13	NS
AFUA_2G16930	Putative succinate:fumarate antiporter	1.62	1.62	1.97	2.08
AFUA_5G10660	Pentatricopeptide repeat protein	2.07	1.80	1.64	NS
AFUA_2G03010	Putative cytochrome C subunit Vb	NS	1.57	NS	NS
	Cell membrane metabolism				
AFUA_8G05600	Putative acyl-CoA thioesterase	2.47	4.75	5.85	4.35
AFUA_4G09190	Putative S-adenosyl-methionine-sterol-C methyltransferase (Erg6)	1.86	2.07	1.60	NS
AFUA_4G03460	SrbB	2.96	2.95	2.00	NS
	Stress response				
AFUA_5G14680	Hydrogen peroxide and gliotoxin induced protein	NS	1.99	5.62	2.84
AFUA_3G00730	Protein with Yap1-dependent induction	NS	NS	1.73	2.45
AFUA_3G12100	Putative trehalase phosphorylase	NS	1.91	3.20	2.73
AFUA_4G03410	Flavohemoprotein FhpA	NS	1.87	2.86	2.29
AFUA_4G04318	Copper metallothioneine CmtA	1.53	1.81	1.80	1.75
	Amino acid catabolism				
AFUA_2G04200	4-hydroxyphenylpyruvate dioxygenase	NS	2.56	3.43	1.82
AFUA_5G14410	Putative cysteine dioxygenase	1.59	3.53	3.27	NS
AFUA_6G08760	Proline oxidase	NS	2.10	2.71	NS
	Glycolytic process / gluconeogenesis				
AFUA_6G07720	Putative phosphoenolpyruvate carboxykinase (AcuF)	2.96	3.00	2.01	NS
AFUA_7G05730	Putative dihydrolipoyl transacetylase	NS	1.57	1.63	NS
	Fermentation				
AFUA_5G06240	Putative zinc-dependent alcohol dehydrogenase AlcC	NS	1.73	4.64	3.67
AFUA_3G11070	Putative pyruvate decarboxylase	NS	2.34	3.89	3.42
	Purine metabolism				
AFUA_2G10520	Putative urate oxidase	NS	1.89	3.34	2.55
	Heme biosynthesis				
AFUA_1G07480	Coproporphyrinogen III oxidase	NS	1.71	2.76	2.30
	Amine metabolism				
AFUA_3G14590	Copper/quinone-containing amine oxidase	NS	NS	2.44	NS
	Others/Unknown				
AFUA_1G03610	Fungoglobin FglA	NS	NS	2.25	2.51
AFUA_1G09030	Protein of unknown function	NS	2.77	4.43	3.00
AFUA_3G03280	Putative FAD binding monooxygenase	NS	1.58	2.56	4.28
AFUA_1G16564	DUF455 domain protein	NS	NS	1.61	NS

This article is protected by copyright. All rights reserved.

Accepted Article

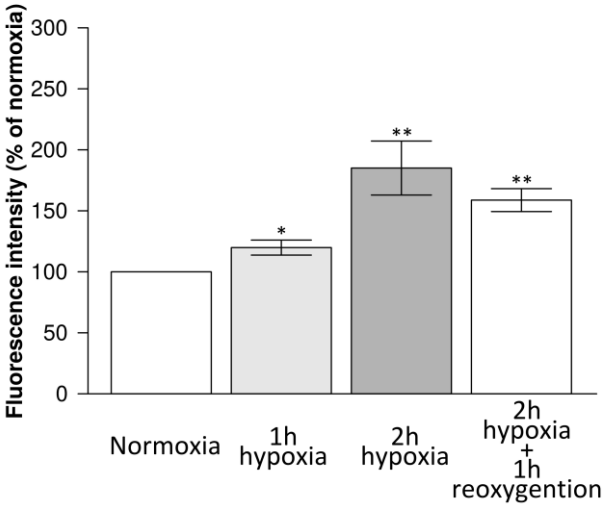

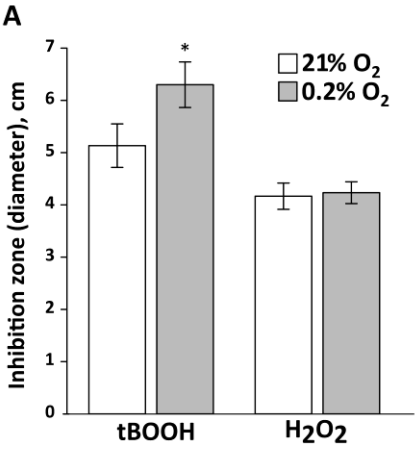

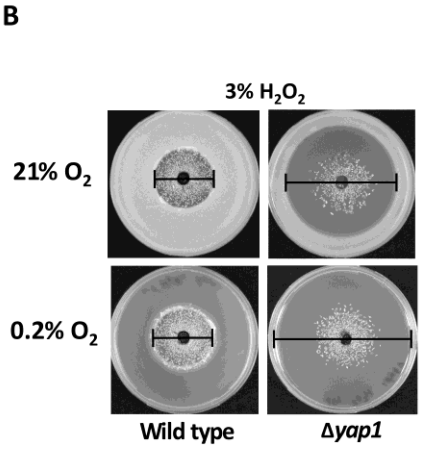

This article is protected by copyright. All rights reserved.

Accepted Article

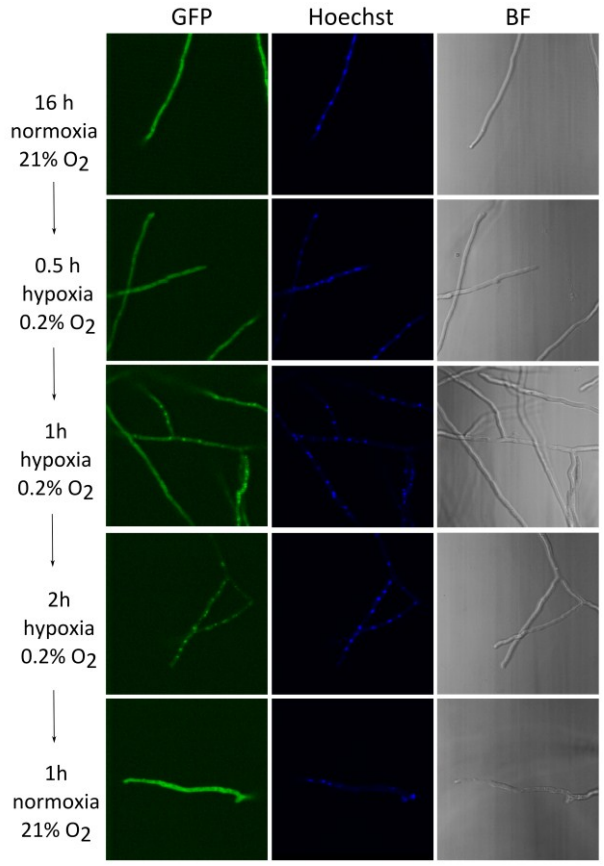

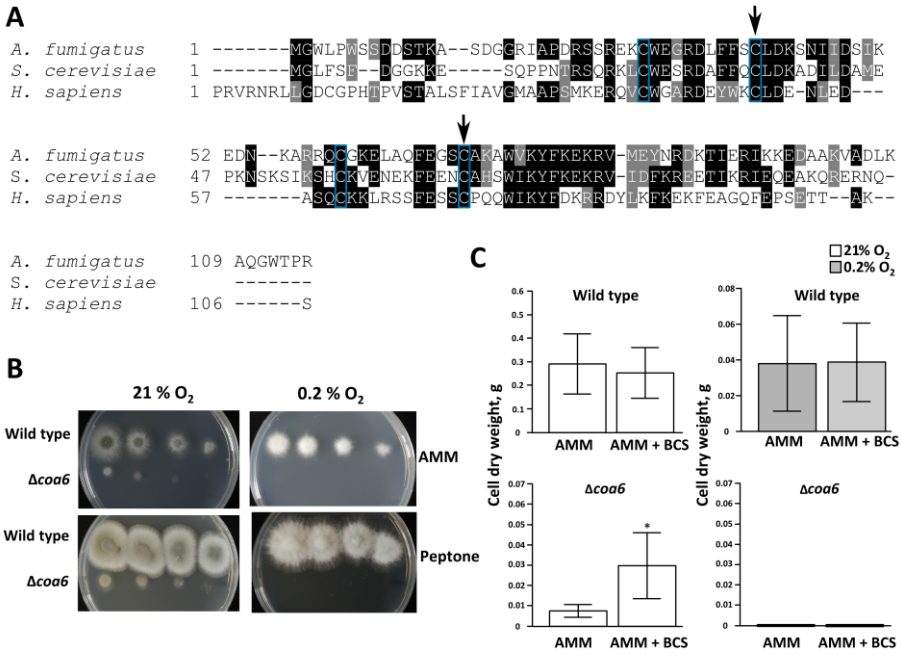

This article is protected by copyright. All rights reserved.